Nonlinear dynamics of classical Heisenberg chains

V. Constantoudis and N. Theodorakopoulos
Theoretical and Physical Chemistry Institute, National Hellenic Research Foundation, Vasileos Constantinou 48, GR-116 35 Athens, Greece
(Received 10 September 1996)

The maximum Lyapunov exponent (MLE) is evaluated as a function of temperature in the isotropic Heisenberg chain. At low temperatures the MLE varies almost quadratically with temperature; it corresponds closely with $\tau_{1/2}^{-1}$, the rate at which the local self-correlation decays to half its initial value. At higher temperatures, the MLE saturates at a value close to 1/2 in the limit of large chain lengths. The strong stochasticity threshold (defined by the change of slope of the MLE) parallels closely the transition from predominantly ballistic to predominantly diffusive behavior of the self-correlation and the concomitant steep increase in $\tau_{1/2}^{-1}$. The complete Lyapunov spectrum has been derived for a chain of 18 spins; deviations from linearity occurring at infinite temperature suggest that the chaoticity of the system is incomplete. Finally, it is suggested that a systematic study of finite-size effects might be useful in deciding the issue of anomalous versus conventional spin diffusion. [S1063-651X(97)05205-7]

PACS number(s): 05.45.+b, 75.10.Hk, 75.40.Gb, 75.40.Mg

I. INTRODUCTION

The classical Heisenberg chain captures many salient features of real magnets. Previous studies [1–11] of its dynamics have focused on the spatially Fourier-transformed autocorrelations, mainly motivated by the need to explain the results of inelastic neutron scattering experiments. At low and intermediate temperatures, the quantity of interest

$$C_q(t) \equiv \langle \vec{S}_q(t) \cdot \vec{S}_{-q}(0) \rangle, \tag{1.1}$$

where $\vec{S}_q(t) \equiv (1/\sqrt{N}) \Sigma_{l=1}^{N} e^{-iql} \vec{S}_l(t)$, or, alternatively, its Fourier transform $\tilde{C}_q(\omega)$ was found to be dominated by spin-wave peaks, whose width increased with increasing temperature. More recent work has emphasized the infinite-temperature aspect: By making use of large-scale numerical simulations, various groups [12–19] have tried to determine whether the (diffusive) hydrodynamics holds exactly in the isotropic case.

Alternatively, it is possible to view the Heisenberg chain as a nonlinear dynamical system and try to exploit concepts and methods developed in the context of dynamical systems. The temperature in this case plays a key role: It is the parameter that tunes the system's behavior from complete (or nearly complete) integrability to fully developed chaos. The most reliable diagnostic tool in order to characterize the degree of intrinsic instability of a nonlinear system with many degrees of freedom is the spectrum of Lyapunov exponents. Calculations of the maximum Lyapunov exponent (MLE) λ_1 in key lattice nonlinear models [Fermi-Pasta-Ulam (FPU) β and ϕ^4] for varying values of the energy density ϵ reveal the existence of a critical value ϵ^*, where the behavior of λ_1 changes. The critical value is independent of the number of degrees of freedom N in the system and is not related to the transition towards ergodic behavior (the ergodic threshold is at lower values of ϵ and tends to zero as $N \to \infty$); it has been attributed to the transition from phase-space diffusion *along* resonances to one *across* resonances [strong stochasticity threshold (SST)] [20–22].

In addition to the MLE, the dependence of the full spectrum of Lyapunov exponents on the energy density has been studied [23,24]. It has been found that, as the integrable limit is approached, only a few of the Lyapunov exponents reflect the chaotic behavior; the rest are relatively small. In contrast, as chaos becomes complete, the Lyapunov spectrum becomes almost linear.

This work presents results for the MLE, the Lyapunov spectrum, and their temperature dependence; in order to facilitate the synthesis between the nonlinear dynamics and the condensed-matter perspectives, we have also calculated the local self-correlations of the spin density. Although the latter quantity does not offer the Fourier resolution needed in the context of detailed studies of transport phenomena and hydrodynamic modes, it is less fluctuation sensitive and better suited to provide reliable data for studying the basic time scales involved, i.e., (i) the short times characterizing the regular decay of correlations; (ii) the intermediate times over which memory is lost (and chaos established), best defined in terms of the decay of self-correlation to half its original value; and (iii) the long times where diffusive behavior dominates. Our results demonstrate that, at low temperatures, the inverse of the MLE, the Lyapunov time, is essentially identical to the time scale (ii) (cf. above). Moreover, our Lyapunov data reveal the existence of a SST that roughly parallels the transition from spin-wave- to diffusion-dominated regime.

The paper is structured as follows. Section II introduces some necessary background on the statistical mechanics of finite chains and discusses the dependence of the MLE and the Lyapunov spectrum on the temperature, the size of the chain, and the type of the interaction. Section III presents results on the autocorrelation function (including a discussion of finite-size effects useful in analyzing long-time data), along with comments on the correspondence between parts

of dynamical information contained in MLE and autocorrelations. Section IV summarizes our basic conclusions.

II. LYAPUNOV EXPONENTS

The dynamics of the classical, isotropic, ferromagnetic, Heisenberg chain is determined by the spin equations of motion

$$\frac{d\vec{S}_i}{dt}=\vec{T}_i(\{\vec{S}_j\})\equiv-\vec{S}_i\times\nabla_{\vec{S}_i}H=\vec{S}_i\times(\vec{S}_{i-1}+\vec{S}_{i+1}),i=1,\ldots,N, \tag{2.1}$$

where $H=-\Sigma_i^N\vec{S}_i\cdot\vec{S}_{i+1}$ and the chain is subjected to periodic boundary conditions $\vec{S}_{N+1}\equiv\vec{S}_1$. It may be remarked in passing that there is an alternative, equivalent formulation of classical spin dynamics, in terms of the canonical variables $p_i\equiv S_i^z$ and $\phi_i=\arctan(S_i^y/S_i^x)$; we have not used this version of the dynamics, in spite of its obvious appeal (smaller number of equations, symplectic structure), because it leads to numerical instabilities (large rates of change) every time a spin becomes parallel to the z axis. On the other hand, the spin dynamics described by the $3N$ equations (2.1) is intrinsically slower than particle dynamics (presumably due to the N conservation laws that express the constancy—N.B. not a constraint—of the spin vectors' magnitude); this imposes an additional limitation on the size of spin rings that can be studied within finite computation times.

For $N\geqslant 3$, there are three independent integrals of motion that are in involution $(H,S_{\rm tot}^z=\Sigma_i^N S_i^z,\vec{S}_{\rm tot}^2)$; in addition, for $N=4$ the quantity $\vec{S}_1\cdot\vec{S}_3$ (or $\vec{S}_2\cdot\vec{S}_4$) is also an independent integral of motion. Thus the ring with $N\leqslant 4$ is completely integrable. For $N>4$ there are $N-3$ positive Lyapunov exponents.

We want our Lyapunov calculations to reflect the system's behavior at a given temperature. Practically, this is done as follows: We compute (theoretically) the canonical averages at temperature T [25,26], $\langle H\rangle_{N,T}$, $\langle S_{\rm tot}^2\rangle_{N,T}$ $(\langle S_{\rm tot}^z\rangle_{N,T}=0)$, and choose initial conditions for the spins that satisfy $H=\langle H\rangle_{N,T}$, $S_{\rm tot}^2=\langle S_{\rm tot}^2\rangle_{N,T}$, and $S_{\rm tot}^z=0$. The Lyapunov exponents calculated in this manner can be considered typical of the dynamical instability at the ''temperature'' T. It should be noted at this point that, from our point of view, there is nothing special about infinite temperature, i.e., the values given below for infinite temperature were obtained from runs with initial conditions $H=0$ and $S_{\rm tot}^2=N$.

The determination of Lyapunov spectra of Eq. (2.1) is based on the method of Benettin *et al.* [27,28], as implemented by Wolf *et al.* [29] and Mutschke and Bahr [24] for particles on a lattice. The scheme involves solving Eq. (2.1), along with the linearized equations of motion

$$\frac{d\,\delta S_{i\alpha}^{(\mu)}}{dt}=\sum_{j=1}^{N}\sum_{\beta=x,y,z}\frac{\partial T_{i\alpha}}{\partial S_{j\beta}}\delta S_{j\beta}^{(\mu)},\quad \mu=1,\ldots,M, \tag{2.2}$$

where M is equal to the number of Lyapunov exponents computed and $I_i^{(\mu)}\equiv\delta\vec{S}_i^{(\mu)}\cdot\vec{S}_i$ vanishes for all i and μ and at all times. [N.B. At $t=0$ this is true by the definition of the tangent space, i.e., it is reflected in the choice of the M linearly independent initial conditions. At later times, the value of $I_i^{(\mu)}$ remains constant; this constancy is not a constraint, but a ''conservation law'' of the joint dynamical evolution in phase and tangent space, as defined by Eqs. (2.1) and (2.2). Hence, in the numerical simulation $I_i^{(\mu)}$ vanishes within numerical error, as is the case with all conservation laws.]

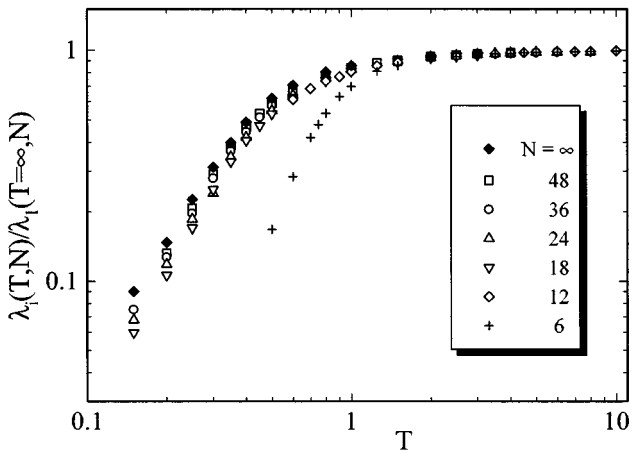

FIG. 1. Maximum Lyapunov exponent as a function of temperature for isotropic Heisenberg chains of different sizes.

Integration of Eqs. (2.1) and (2.2) is performed by a fourth-order Runge-Kutta method with adaptive step size control. The time interval between successive Gram-Schmid orthogonalizations was $\Delta t=0.1$ and determination of the MLE took approximately 1.5×10^6 steps; computation of the full Lyapunov spectrum was restricted to 0.5×10^6 steps. The statistics of values of the Lyapunov exponents obtained during the last quarter of the integration interval showed that, in all cases, the (relative) standard deviation was less than 10^{-3} for the MLE and less than 5×10^{-3} for the other exponents. The values of the three constants of motion were monitored during the course of integration; the relative error did not exceed 5×10^{-6}.

Initially, we computed the MLE λ_1 for rings of size $N=12,24,36,48$ and temperatures between 0.15 and ∞ (cf. above). We observe that, although the overall form of $\lambda_1(T)$ seems to be the same for all N, the values depend somewhat on ring size. Furthermore, we exploit the fact that the MLE approaches a constant value as the temperature tends to infinity, in order to produce a ''reduced'' plot of the temperature dependence of the MLE (Fig. 1). The values of the infinite-temperature MLE's as a function of $1/N$ are shown separately in Fig. 2.

The main feature of $\lambda_1(T)$, for all values of N, is the smooth change of slope that characterizes the transition from the low- to the high-temperature regime. This seems to be a generic feature of Hamiltonian systems with a large number of degrees of freedom. It has been observed in the $O(2)$ Heisenberg model [30], the FPU β model, and the ϕ^4 model [20–22] and has been correlated with the appearance of a SST [20–22], i.e., a critical value of the energy density ϵ_c (or the temperature $T_{\rm cr}$), above which rapid diffusion in phase

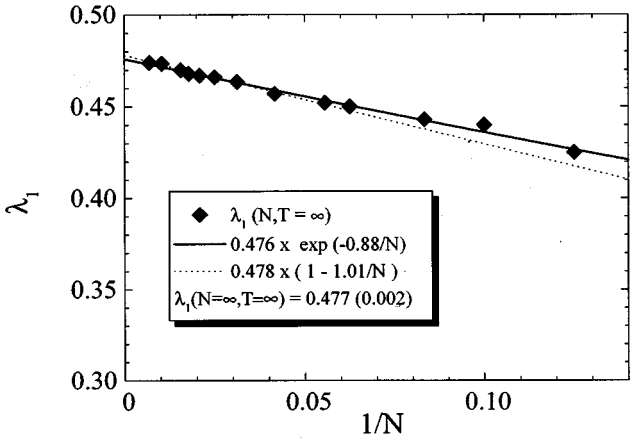

FIG. 2. Size dependence of the maximum Lyapunov exponent at infinite temperature.

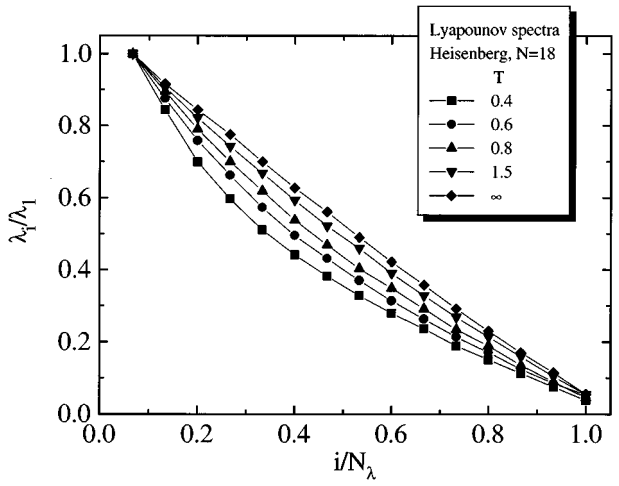

FIG. 3. Spectrum of Lyapunov exponents at high and intermediate temperatures.

space can occur as a result of strong overlap of resonances in the stochastic web. Diffusion in this case takes place across resonances, in contrast to what happens for $\epsilon<\epsilon_c$, where (Arnold-like [31]) diffusion can take place only along resonances. Orbits in the case of Arnold diffusion are more ''tortuous'' and less chaotic. The SST thus signals the destruction of the stochastic web.

A rough estimate of the crossover temperature can be obtained by the intersection of the straight line that describes the low-temperature ($T<0.4$) asymptotic behavior of $\lambda_1(T)$, with the infinite-temperature asymptote. For $N=48$ we estimate $T_{\rm cr}=0.55$. At low temperatures, we find that $\lambda_1(T)\sim T^{1.9}$; we will return to the above estimates of the crossover temperature and the power-law behavior of the MLE in Sec. III in order to correlate these findings with autocorrelation data.

A more complete description of chaotic behavior is provided by the full spectrum of Lyapunov exponents. Computations in a variety of Hamiltonian systems have shown that as the integrable limit is approached, the number of Lyapunov exponents effectively responsible for chaotic behavior decreases; in other words, the curvature of the function $\lambda_i(i/N_\lambda)$ (where N_λ is the total number of nonzero Lyapunov exponents) increases. Conversely, as complete chaos evolves, the Lyapunov spectrum (LS) becomes nearly linear. (Compare the numerical evidence given by Livi *et al.* [23] that the LS generated by the application of random matrices is linear.) The curvature of the LS could thus provide an alternative measure of chaoticity.

In order to pursue this question further, we studied the LS for a chain with $N=18$ over the whole temperature range used in the MLE computations. Results above $T=0.4$ are consistent with the simple picture presented above, i.e., a monotonic decrease of the spectrum's curvature with increasing temperature (cf. Fig. 3). It should be noted, however, that even in the infinite-temperature limit, there is a significant deviation from linearity. It would be interesting to explore whether this is a finite-size effect, but our computational capacities do not allow us to compute LS of larger chains. On the basis of our findings, we tend to attribute the deviations from linearity to residual nonrandom dynamics; in a spin system this suggests the presence of spin waves that persist up to infinite temperature. This argument is supported by the LS of Heisenberg chains with random (i.e., $H=-\Sigma_i^N J_i\vec{S}_i\cdot\vec{S}_{i+1}, J_i=\pm 1$; cf. [13]) and alternating interactions [$J_i=(-1)^i$; cf. [13]], which show stronger deviations from linearity (especially the alternating case) (Fig. 4) and concomitant stronger signatures of short-time spin-wave-like dynamics (cf. the next section).

Results below $T=0.4$ seem to reverse even the general trend: Although $\lambda_1(T)$ continues to decrease, the spectrum's curvature, as measured by, e.g. ,

$$\frac{\langle|\Delta\lambda|\rangle}{\lambda_1}=\frac{1}{N_\lambda}\sum_{i=1}^{N_\lambda}\left|\lambda_i-\frac{N_\lambda-i+1}{N_\lambda}\lambda_1\right|, \tag{2.3}$$

stops increasing and in fact shows signs of a decrease (Fig. 5). Thus the curvature at $T=0.2$ and $T=0.5$ hardly differ; maximum curvature appears at $T=0.4$. [It is interesting to note in this context that $T=0.4$ is also the maximum temperature for which $\lambda_1(T)$ exhibits power-law behavior.] In

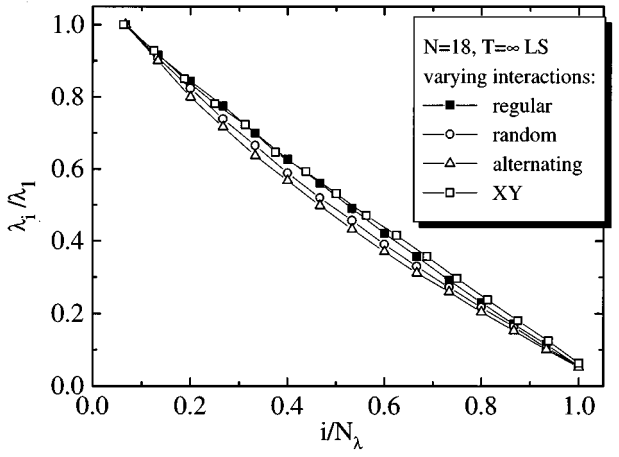

FIG. 4. Lyapunov spectrum for three types of isotropic Heisenberg chains, with (i) regular ferromagnetic, (ii) random, (iii) alternating nearest-neighbor interactions.

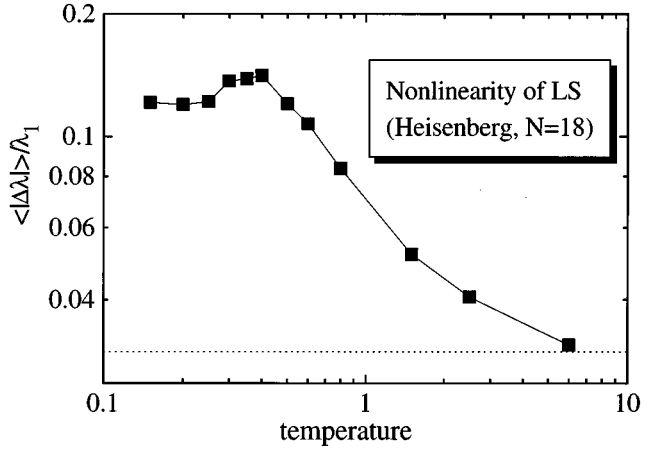

FIG. 5. Deviation of the Lyapunov spectrum from linearity [Eq. (2.3)] vs temperature.

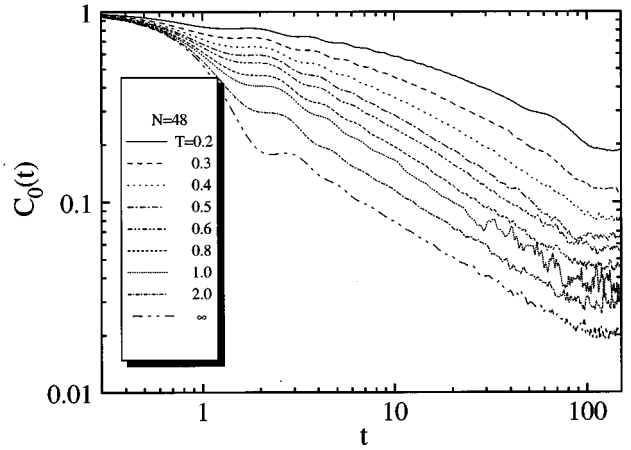

FIG. 6. Autocorrelation function of the classical Heisenberg ring ($N=48$) at different temperatures.

conclusion, it appears that the curvature of the LS can provide a complementary measure of the chaoticity at moderate and high temperatures.

III. AUTOCORRELATION FUNCTIONS

As mentioned in the Introduction, the spectrum of dynamical correlations has been extensively studied in connection with underlying spin-wave dynamics (at low temperatures), or with spin diffusion (at infinite temperature). In this work, we focus on those characteristics of the dynamical autocorrelations that are most likely to relate to the observed Lyapunov behavior. More specifically, we deal with the following issues related to the local spin-spin autocorrelation function:

$$C(t)=\frac{1}{N}\sum_{i=1}^{N}\langle\vec{S}_i(t)\cdot\vec{S}_i(0)\rangle: \tag{3.1}$$

(i) the short- and intermediate-time behavior of $C(t)$ and its relationship with the MLE; (ii) the determination of the crossover temperature, above which $C(t)$ becomes diffusion dominated, and the relationship to the SST; and (iii) infinite-time, finite-size characteristics of $C(t)$.

Our calculation of Eq. (3.1) at a given temperature proceeds as follows. An initial condition is chosen, with $E, S^z_{\rm tot}, S^2_{\rm tot}$ equal to their respective average values at that temperature. The system is left to evolve according to Eq. (2.1) and a time average over the orbit is taken.

Figure 6 summarizes the time dependence of $C(t)$ for a variety of temperatures and $N=48$. Finite-size effects can best be isolated at infinite temperature (Fig. 7). Finally, in order to investigate the dependence of $C(t)$ on the type of the interaction, we have repeated the infinite temperature calculation for the two chains mentioned in Sec. II, namely, the alternating and the random exchange chain; results are shown in Fig. 8 for $N=18$. On the basis of our findings, we now discuss the three issues described above.

A. Short- and intermediate-time dynamics and Lyapunov exponents

The behavior of $C(t)$ at short times is well accounted for in terms of a Gaussian $\exp[-\frac{1}{2}(t/\tau_1)^2]$, where $\tau_1^{-1}=(\langle\omega^2\rangle)^{1/2}$ can be obtained to a good approximation from a second-order moment expansion. This short-time decay represents the random superposition of regular motion in phase space (parabolic decay of the cosine functions); its duration is at all temperatures shorter than the inverse Lyapunov time (cf. Fig. 9). Also plotted in Fig. 9 is $\tau_{1/2}^{-1}$, the (inverse) time it takes for the autocorrelation to decay to 1/2, and the Lyapunov exponent. At low temperatures, the dependence of $\tau_{1/2}^{-1}$ on temperature roughly parallels that of the MLE; in fact, the two numbers are rougly equal in magnitude. This means that the decay of the $C(t)$ to half its original value fully reflects the system's chaotic nature. At this point, it is interesting to note that the asymptotic power law followed by the MLE (cf. Sec. II) makes it proportional to the square of the inverse correlation length; this is exactly the crossover time characterizing the transition from spin-wave-like to diffusive behavior, at wave vectors comparable to the inverse correlation length.

At very high temperatures, the half-time becomes very short; its inverse exceeds the MLE. In fact, $\tau_{1/2}^{-1}=\tau_1^{-1}/(2\ln 2)^{1/2}$ holds, indicating that the decay is now dominated by the regular parabolic decay. It is interesting to note

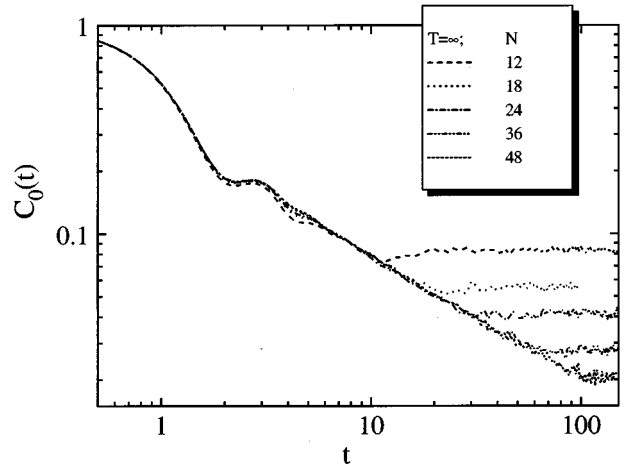

FIG. 7. Size dependence of the autocorrelation function of the classical Heisenberg ring at infinite temperatures.

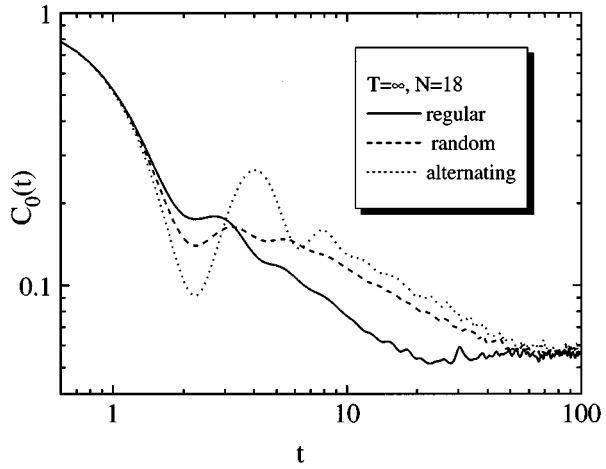

FIG. 8. Autocorrelation function at infinite temperature for three types of classical Heisenberg rings, with regular, random, and alternating nearest-neighbor interactions (cf. text), respectively.

that the numerical value of the MLE allows this type of behavior. If the MLE had a larger value, there would be no parabolic decay and no plateau preceding the onset of diffusion. The steep change in $\tau_{1/2}^{-1}$ between $T=0.6$ and 0.8 reflects the fact that, at this temperature, the height of the broad plateau in $C(t)$ (cf. Fig. 6) is in the vicinity of 1/2.

B. Spin diffusion vs strong stochasticity thresholds

At infinite temperature, the long-time behavior of the spin-spin autocorrelations is expected to be dominated by spin diffusion. In one dimension this implies $C(t)\propto t^{-1/2}$. Sidestepping the issue of anomalous vs conventional diffusion for the moment (cf. below), we will consider, for our purposes, diffusive behavior to be defined by a power-law decay of $C(t)$; we are principally interested in determining the temperature dependence of diffusive behavior and in following its correlation with the onset of fully developed chaos.

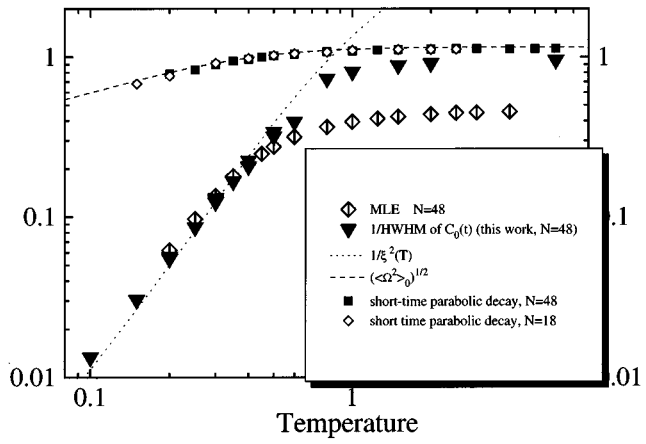

FIG. 9. Summary of the temperature dependence of the basic time scales that govern the dynamics of the autocorrelation function $C_0(t)$. The upper curve represents the width τ_1^- of the Gaussian fit to the short-time (nonchaotic) parabolic decay of the autocorrelation function. The inverted triangles represent the halflife of the autocorrelation; note the steep increase around $T=0.6$. Also plotted are the values of the maximum Lyapunov exponent.

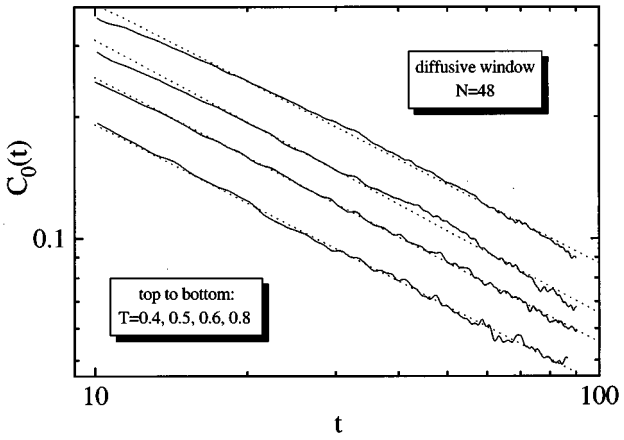

FIG. 10. Long-time behavior of $C_0(t)$ at temperatures $T=0.4,0.5,0.6,0.8$ (from top to bottom); note the onset of the power-law behavior around $T=0.6$.

It can be seen from Fig. 6 that the transition from ballistic to diffusive behavior occurs somewhere between $T=0.4$ and $T=0.8$. In order to make this clearer, we present in Fig. 10 the time segment $10\leqslant t\leqslant 90$ and attempt to fit to a straight line. Deviations are evident for $T=0.4$ and $T=0.5$; they are hardly visible at $T=0.6$. It is reasonable to claim that the latter temperature signals the crossover to the diffusion-dominated regime. It should be noted that the strong stochasticity threshold (cf. Sec. II) also occurs at that temperature. It therefore appears that the transition from (phase-space) diffusion along resonances to (phase-space) diffusion across resonances coincides with the transition from spin-wave- to diffusion-dominated dynamics. In order to understand this phenomenon better, it should be remembered that the destruction of the stochastic web is not a sudden process and does not necessarily occur homogeneously in phase space; this is best demonstrated by the smooth change of slope of $\lambda_1(T)$ in the isotropic Heisenberg case, as compared with the FPU β or ϕ^4 models. The scenario taking into account the numerous investigations of (space and time) Fourier-transformed spin-spin correlations seems to proceed as follows. At relatively low temperatures, only those regions of the stochastic web are destroyed that correspond to spin waves of low wave numbers. As the temperature increases, the destruction of the web extends over wider regions, allowing diffusive behavior across resonances in phase space. This should not be construed to imply that all spin-wave modes are overdamped; indeed, there is evidence for the persistence of some spin-wave modes (with wave vectors near the Brillouin-zone edge) up to very high temperatures [11,15].

The exponent of the power law that characterizes $C(t)$ remains temperature independent from the onset of its appearance. Furthermore, its value, 0.6, appears to be independent of the ring's length.

Traces of the anomaly in the diffusion exponent can be seen in Fig. 9, where $C(t)$ is plotted for regular, random, and alternating chains with $N=18$. The regular chain has less structure at short and intermediate times and appears to decay faster at long times.

C. Long-time characteristics: Finite-size effects

It can be seen from Figs. 6–8 that autocorrelations do not decay indefinitely. After a finite time t_∞, $C(t)$ saturates at a

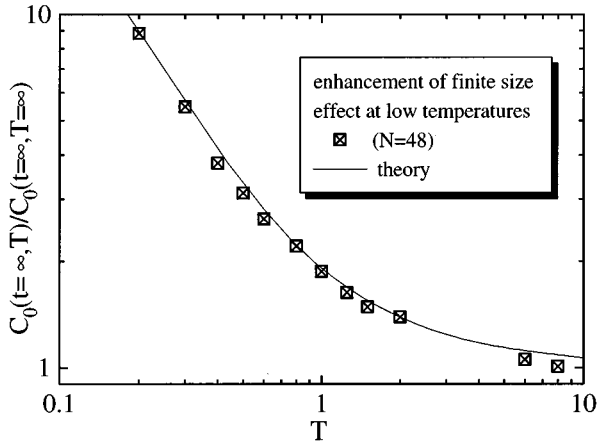

FIG. 11. Limiting value of the spin-spin autocorrelation as $t\to\infty$, plotted as a function of temperature, for $N=48$. Also shown is the prediction of Eq. (3.5).

finite value C_∞. Both constants t_∞ and C_∞ are size dependent; accordingly, a study of the size dependence may prove revealing for the system's approach to equilibrium in the thermodynamic limit.

Conservation of the total magnetization

$$\vec{S}(t)\equiv\sum_{i=1}^{N}\vec{S}_i(t)=\vec{S}(0) \tag{3.2}$$

implies that the correlation functions

$$C^{(m)}(t)=\frac{1}{N}\sum_{i=1}^{N}\langle\vec{S}_{i+m}(t)\cdot\vec{S}_i(0)\rangle \tag{3.3}$$

satisfy at all times the sum rule

$$\sum_{i=1}^{N}C^{(m)}(t)=\sum_{m}\langle\vec{S}_m(0)\cdot\vec{S}_0(0)\rangle=\frac{1+u}{1-u}, \tag{3.4}$$

where $u=\coth(1/T)-T$. At very long times $t>t_\infty$, spin diffusion ensures that any fluctuation in the initial values is uniformly distributed in the chain, i.e., all terms in Eq. (3.3) contribute equally to the sum, and

$$C^{(m)}(t)\approx C_\infty=\frac{1}{N}\frac{1+u}{1-u},\quad m=1,\ldots,N. \tag{3.5}$$

The above reasoning is independent of the particular type of chain and depends solely on the isotropic property; Fig. 8 confirms this explicitly by showing that $C(t)$ in the ferromagnetic, random, and alternating chains all converge to the same limiting values. It is already apparent from Fig. 6 that this type of finite-size effect increases as the temperature is lowered. The plot shown in Fig. 11 confirms that this increase of C_∞ closely follows Eq. (3.5).

The size dependence of t_∞ offers additional insight into the long-time, diffusion-dominated dynamics of the system. It is instructive to analyze the data in two different ways: plotting $t>t_\infty$ vs N on a double logarithmic scale [Fig. 12(a)] shows that the data for the chains considered in this work are consistent with

$$t_\infty\propto N^{1.67}; \tag{3.6}$$

such a value might indeed reflect anomalous diffusion with an exponent equal to $1/1.67=0.6$, i.e., in agreement with the

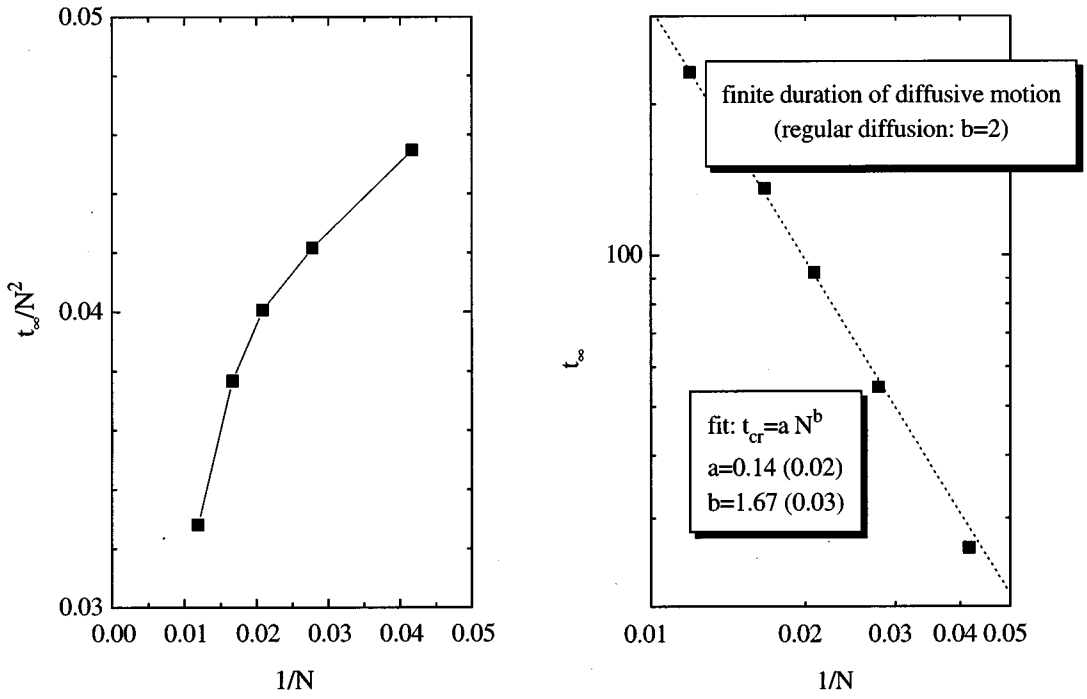

FIG. 12. Right: size dependence of t_∞, the time it takes for the spin-spin autocorrelation to reach its saturation value. The scale is doubly logarithmic and the slope $b=1.67$ corresponds to a spread of a spin fluctuation according to $\langle(\Delta x)^b\rangle\propto t$, i.e., an anomalous diffusion with an exponent $1/b=0.60$ (cf. Ref. [12]). Left: regular diffusion [fit according to Eq. (3.7)] would produce points lying on a straight line.

value originally suggested by Müller [12,13]. Alternatively, it is evident that our results cannot be fitted to the straight line

$$\frac{t_\infty(N)}{N^2} = a + \frac{b}{N} \tag{3.7}$$

[Fig. 12(b)] [which would imply a loss of memory due to (regular) diffusion, including (analytic) corrections that become negligible in the thermodynamic limit]. The above procedure distinguishes between Eqs. (3.6) and (3.7) and can be used, in principle, as a *direct* test for anomalous diffusion; unfortunately, the chain lengths necessary for a definitive test are beyond our present computational capabilities. In view of the current lack of (general as well as internal) consensus between theoretical approaches (conventional hydrodynamics vs ''refined mode coupling'' [32], which proposes anomalous diffusion with an exponent 2/5) and extensive numerical simulation results (which suggest that regular diffusion may [15] or may not [19] prevail at longer times and larger chains) such a (definitive) test appears highly desirable.

IV. CONCLUDING REMARKS

We have shown that the information contained in the Heisenberg chain's Lyapunov exponents may be useful in interpreting the dynamics of the local autocorrelation function. The quantitative agreement between the largest Lyapunov exponent and the inverse half-time of the local self-correlation at low temperatures confirms that both quantities express the time scale involved in the loss of memory occurring in the near-integrable regime. At intermediate temperatures, we have identified the occurrence of the SST with the passage of the autocorrelation dynamics from the spin-wave- to the diffusion-dominated regime. Finally, at infinite temperatures, the deviations of the Lyapunov spectrum from the linear form has been ascribed to the same lack of complete chaos that characterizes autocorrelations; moreover, the relatively small value of the largest Lyapunov exponent, compared with the period of short-wavelength excitations, explains why the latter persist even at infinite temperatures, giving rise to the ''plateau'' feature in the self-correlation.

ACKNOWLEDGMENTS

We wish to thank S. Flach and G. Mutschke for providing us with the particle version of the source code for the calculation of the Lyapunov spectrum.

[1] M.F. Collins and W. Marshall, Proc. R. Soc. London **98**, 367 (1967).
[2] S.W. Lovesey and R.A. Meserve, Phys. Rev. Lett. **28**, 614 (1972).
[3] S.W. Lovesey, J. Phys. C **7**, 2008 (1974).
[4] S.W. Lovesey and J.M. Loveluck, J. Phys. C **9**, 3639 (1976).
[5] M. Resibois and M. deLeener, Phys. Rev. **152**, 305 (1966); **152**, 318 (1966).
[6] M. Blume and J. Hubbard, Phys. Rev. B **1**, 3815 (1970).
[7] N.A. Lurie, D.L. Huber, and M. Blume, Phys. Rev. B **9**, 2171 (1974).
[8] J.M. Loveluck and C.G. Windsor, J. Phys. C **11**, 2999 (1978).
[9] *Physics in One Dimension*, edited by J. Bernasconi and T. Schneider, Springer Series in Solid State Sciences Vol. 23 (Springer-Verlag, Berlin, 1981).
[10] G. Reiter and A. Sjölander, J. Phys. C **13**, 3027 (1980).
[11] M. Takahashi, J. Phys. Soc. Jpn. **52**, 3572 (1983).
[12] G. Müller, Phys. Rev. Lett. **60**, 2785 (1988).
[13] G. Müller, Phys. Rev. Lett. **63**, 813 (1989).
[14] R.W. Gerling and D.P. Landau, Phys. Rev. Lett. **63**, 812 (1989).
[15] R.W. Gerling and D.P. Landau, Phys. Rev. B **42**, 8214 (1990).
[16] R.W. Gerling and D.P. Landau, Phys. Rev. B **41**, 7139 (1990).
[17] J.-W. Liu, N. Srivastava, V.S. Viswanath, and G. Müller, J. Appl. Phys. **70**, 6181 (1991).
[18] M. Böhm, R.W. Gerling, and H. Leschke, Phys. Rev. Lett. **70**, 248 (1993).
[19] O.F. de Alcantara Bonfim and G. Reiter, Phys. Rev. Lett. **69**, 367 (1992); **70**, 249 (1993).
[20] M. Pettini and M. Landolfi, Phys. Rev. A **41**, 768 (1989).
[21] M. Pettini and M. Cerruti-Sola, Phys. Rev. A **44**, 975 (1991).
[22] L. Casetti and M. Pettini, Phys. Rev. E **48**, 4320 (1993).
[23] R. Livi, A. Politi, S. Ruffo, and A. Vulpiani, J. Stat. Phys. **40**, 147 (1987).
[24] G. Mutschke and U. Bahr, Physica D **69**, 302 (1993).
[25] M.E. Fisher, Am. J. Phys. **32**, 343 (1964).
[26] G.S. Joyce, Phys. Rev. **155**, 478 (1967).
[27] G. Benettin, L. Galgani, and J.-M. Strelcyn, Phys. Rev. A **14**, 2338 (1976).
[28] G. Benettin, L. Galgani, A. Giorgilli, and J.-M. Strelcyn, Mechanica **15**, 9 (1980).
[29] A. Wolf, J.B. Swift, H.L. Swinney, and J.A. Vastano, Physica D **16**, 285 (1985).
[30] P. Butera and G. Caravati, Phys. Rev. A **36**, 962 (1987).
[31] V.I. Arnold, Dokl. Akad. Nauk SSSR **156**, 9 (1964) [Sov. Math. Phys. Dokl. **5**, 581 (1965)].
[32] S.W. Lovesey and E. Balcar, J. Phys. Condens. Matter **6**, 1253 (1994).